Natural Product Communications
Volume 19(12): 1–12

DOI: 10.1177/1934578X241310020
journals.sagepub.com/home/npx

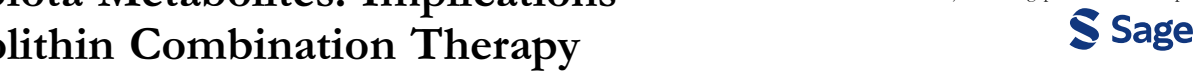

Enhancing the Efficacy of Radiotherapy in Gastric Adenocarcinoma Cells by Gut Microbiota Metabolites: Implications for Urolithin Combination Therapy

Abdolreza Ahmadi[1], Fatemehsadat Hosseini[1], Hassan Ostadi[1], Hamid Gholamhosseinian[2], Milad Iranshahy[3] and Fatemeh B. Rassouli[1]

Abstract

Background: Gastric adenocarcinoma (GA) ranks as the fourth leading cause of cancer-related mortality. The clinical effectiveness of radiotherapy in GA patients is often limited by the development of radiation resistance. Urolithins, which are metabolites produced by gut microbiota from ellagitannins, possess good bioavailability and exhibit beneficial pharmaceutical properties. The aim of present study was to determine whether urolithins can enhance the effects of ionizing radiation (IR) on GA cells for the first time. **Methods:** Urolithins were synthesized and MKN-45 cells were pretreated with UroA, UroB, and mUroA for 24, 48 and 72 h, followed by 400, 600 and 800 cGy IR exposure. After recovery, the viability of the cells was evaluated by resazurin assay, and the mode of interaction between urolithins and IR was determined. Then, interactome mapping and gene set enrichment analyses were performed. Upon validating CHEK1 expression in GA tissues and MKN-45 cells, molecular docking was conducted to predict the interaction of urolithins with CHK1. **Results:** Pretreatment with urolithins significantly decreased viability upon radiotherapy. The most considerable decrease in the cell viability was observed after 400 cGy IR exposure. In comparison to the control treatments, 24 h pretreatment with UroA and mUroA significantly ($p < .0001$) reduced cell viability to 57.4% and 62.8%, respectively. In addition, 48 h pretreatment with UroA and mUroA significantly ($p < .001$) reduced viability to 69.7% and 72.7% after exposure to 400 cGy IR, respectively. Upon 72 h pretreatment with urolithins, only mUroA induced synergistic effects with 400 cGy IR. *In silico* analyses highlighted CHK1 as one of the main proteins involved in the response to IR-induced DNA damage, showing overexpression in GA samples and MKN-45 cells. Additionally, molecular docking revealed favorable interactions between urolithins and CHK1. **Conclusion:** Present study highlights the notable synergistic effects of urolithins in combination with IR, indicating their potential to improve therapeutic outcomes.

Keywords

Urolithins, ionizing radiation, gastric adenocarcinoma, ellagic acid derivatives, gut microbiota metabolites, CHK1

Received: September 11th, 2024; Accepted: December 10th, 2024.

Introduction

Gastric adenocarcinoma (GA) is the fifth most frequent type of neoplasm worldwide, and the fourth most common cause of cancer-related deaths.[1] The incidence of GA shows considerable geographic variation, with over three-quarters (75.3%) of all cases occurring in Asia. Notably, 86.7% of these cases are found in more developed regions. This disparity in incidence is primarily attributed to differences in the prevalence of genetic and environmental risk factors such as *Helicobacter pylori* infection, dietary habits, and smoking.[2,3] During the recent years, notable advancements have been made in early diagnosis of GA, including microfluidic chips and multiplexed immunofluorescence staining.[4,5] Nevertheless, the survival rate for patients with advanced GA remains less than one year.[6] One significant contributor to GA-related mortality is peritoneal metastasis that occurs in over 50% of patients,[7] which made it difficult to cure the disease with conventional approaches.

[1]Novel Diagnostics and Therapeutics Research Group, Institute of Biotechnology, Ferdowsi University of Mashhad, Mashhad, Iran
[2]Department of Medical Physics, Faculty of Medicine, Mashhad University of Medical Sciences, Mashhad, Iran
[3]Biotechnology Research Center, Pharmaceutical Technology Institute, Mashhad University of Medical Sciences, Mashhad, Iran

Corresponding Author:
Fatemeh B. Rassouli, Novel Diagnostics and Therapeutics Research Group, Institute of Biotechnology, Ferdowsi University of Mashhad, Mashhad, Iran.
Email: behnam3260@um.ac.ir

In addition to surgical intervention, several therapeutic strategies are employed to treat GA, including radiotherapy, systemic chemotherapy and targeted therapy.[8,9] Specifically, use of ionizing radiation (IR) continues to be an essential approach for alleviating symptoms in GA patients, particularly those suffering from gastrointestinal bleeding and pain resulting from distant metastases.[10] In addition, clinical trials established adjuvant chemoradiotherapy as a standard treatment for resected gastric cancer, showing improvements in overall survival and disease-free survival among patients receiving combined treatment.[11,12] However, challenges such as the emergence of resistance and off-target toxicity persist, complicating the treatment of GA.[13] Therefore, there is an urgent demand to enhance the efficacy of radiotherapy by incorporating novel sensitizing agents.

The main mode of action of IR is through direct DNA single- and double-strand breaks, as well as indirect DNA damage from oxidative stress, which disrupt cellular functions.[14] In radioresistant cancer cells, however, proteins involved in the DNA damage response (DDR) are overexpressed, and cell cycle checkpoints are exploited to delay progression through the cycle and allow DNA repair. Checkpoint kinase 1 (CHK1/CHEK1) is a serine/threonine kinase that plays a crucial role in maintaining genomic integrity by coordinating the cellular response to DNA damage. The phosphorylation and activation of CHK1 in response to DNA damage affects key regulatory proteins such as CDC25 and WEE1, enforcing cell cycle arrest to enable DNA repair.[15,16] Since elevated CHK1 expression is detected in various cancers and correlates with poor prognosis and increased tumor aggressiveness, ongoing research aims to delineate optimal combinations of CHK1 inhibitors with existing therapies to improve outcomes for patients with radioresistant phenotype.[17,18]

Contemporary cancer research is focused on identifying natural compounds that are effective, affordable, and safe. One such group of compounds are ellagitannins (ETs), which are hexahydroxydiphenoic acid esters found in abundance in fruits such as pomegranate, berries and nuts. After being consumed, ETs undergo metabolic transformation by gut microbiota, resulting in the production of urolithins with favorable bioavailability.[19,20] In addition to their well-documented antimicrobial, anti-inflammatory, and antioxidant properties, urolithins exhibit significant anticancer activity.[21] For instance, treatment of endometrial and prostate cancer cells with urolithins disrupted P38-MAPK pathway and induced caspase-3-dependent apoptosis.[22,23] More studies on prostate cancer cells revealed that urolithins exerted their anticancer effects by inhibiting the AR/pAKT signaling pathway, activating caspases 3 and 7, and inhibiting EphA2 phosphorylation.[24,25] Additionally, it has been shown that urolithin A (UroA) inhibited growth and induced apoptosis in pancreatic and liver cancer cells by halting AKT phosphorylation, reducing the expression of β-catenin, c-MYC, and CCND1, while increasing the expression of P53 and caspase-3.[26,27] Furthermore, treatment of hepatocellular carcinoma cells with UroA decreased cell proliferation and survival through the induction of P53, P38-MAPK, and caspase-3 expression while reducing ROS levels.[28] In an attempt on cholangiocarcinoma cells, UroA induced autophagy through targeting the AKT/WNK1 axis.[29] In studies involving bladder cancer cells, UroA and urolithin B (UroB) were found to induce apoptosis, inhibit the cell cycle, decrease ROS levels, and increase SOD levels.[30,31] Moreover, research on several colon cancer cell lines demonstrated that UroA and UroB induced apoptosis and cell cycle arrest, upregulated CDKN1A expression, and activated caspases 8 and 9.[32-35] It has also been shown that UroA and UroB reduced the growth and migration of glioblastoma cells via inhibiting the AKT and EGFR pathways.[36] Additionally, anti-metastatic effects of urolithins have been documented in lung, endometrial, nasopharyngeal, brain and colorectal cancer cells.[24,35,37-40] Interestingly, research has demonstrated that urolithins have the potential to improve the efficiency of radiotherapy, chemical drugs and hyperthermia in esophageal, prostate and colon carcinoma cells.[25,41,42]

In light of the pressing need to combat radioresistance in GA, this study aimed to explore the potential of urolithins—UroA, UroB and methyl UroA (mUroA)—to enhance the effects of IR in GA cells for the first time. To achieve this, urolithins were synthesized, and MKN-45 cells were pretreated with UroA, UroB and mUroA, and then exposed to IR. After recovery, cells were assessed for viability, and the mode of interaction between urolithins and IR was determined. For *in silico* analyses, interactome mapping and gene set enrichment analyses were performed. Upon validating CHEK1 expression in GA tissues and MKN-45 cells, molecular docking was conducted to predict the interaction of urolithins with CHK1.

Material and Methods

Synthesis of Urolithins

Urolithins were synthesized by condensation of either resorcinol with the appropriately substituted benzoic acids as previously described.[43] The purity of all three synthesized urolithins was >95%, which was confirmed by thin layer chromatography on silica gel (Merck) using petroleum ether-ethyl acetate as a solvent (Merck). Structural identity was also confirmed by molecular mass and ^{1}H NMR spectra.

The synthesis of mUroA (3-hydroxy-8-methoxy-6H-dibenzo-[b,d]pyran-6-one) was achieved through a reaction involving 2-bromo-5-methoxybenzoic acid (12 g, Merck) and resorcinol (25 g, Merck) under alkaline condition. Then, aqueous $CuSO_4$ (5% w/v, 1.80 ml) was added and the mixture was refluxed, during which mUroA precipitated as a light yellow powder. Upon filtration and washing with cold methanol, pure mUroA was obtained.

For synthesis of UroA (3,8-dihydroxy-6H-dibenzo-[b,d] pyran-6-one), purified mUroA was dissolved in anhydrous dichloromethane (0.5 ml, Merck) and treated with boron tribromide (1 M, Merck) in dichloromethane (0.7 ml, Merck). After filtering the mixture with ethyl acetate (Merck), the solvent was evaporated, yielding pure UroA as a white powder.

Synthesis of UroB (3-hydroxy-6H-dibenzo-[b,d]pyran-6-one) was performed using 2-bromobenzoic acid (Merck), resorcinol and NaOH. The mixture was refluxed and upon addition of aqueous $CuSO_4$, UroB precipitated as a white powder. It was then filtered and washed with cold methanol to achieve pure UroB.

Cell Culture and Treatment

MKN-45 cells, a human GA cell line, were obtained from the Pasteur Institute (Tehran, Iran). This cell line has been derived from a poorly differentiated GA of a 62-year-old Japanese female patient. In addition to being characterized by rapid growth, MKN-45 cells rank fourth among forty-two GA cell lines in terms of CHEK1 expression (https://www.proteinatlas.org/). The cells were cultured in Dulbecco's modified Eagle's medium (Capricorn) supplemented with 10% fetal bovine serum (Gibco), under standard conditions of 37 °C in a humidified atmosphere containing 5% CO_2. The culture medium was changed every two to three days, and cells were passaged upon reaching confluency using 0.25% trypsin-1 mM EDTA (Betacell).

For cell treatment, at first stock solutions of UroA (87.6 mM), UroB (94.2 mM) and mUroA (82.3 mM) were prepared using dimethyl sulfoxide (DMSO, Merck) as solvent. To identify the optimal concentration of urolithins for combinatorial treatments with IR, cells were initially treated with 25, 50 and 100 μM of each urolithin for three consecutive days. After determining the IC_{50} value of all agents, 75 μM was established as a sublethal dose to be used for pretreatment prior to radiotherapy. For combinatorial treatments, cells were subjected to 75 μM UroA, UroB and mUroA for 24, 48 and 72 h, and then exposed to different doses of IR (400, 600, and 800 cGy) using the Elekta Compact™ linear accelerator (Crawley). To note, selection of 400, 600 and 800 cGy for cell radiotherapy was informed by established protocols in radiation oncology, which suggest that these doses are effective for inducing cellular damage while allowing for assessment of potential synergistic effects with radiosensitizers.[44] Following 48 and 24 h recovery, cell viability assay was performed. Noteworthy, untreated cells and cells pretreated with 0.5% DMSO and exposed to IR were considered as controls.

Viability Assay and Interaction Mode Determination

Viability of cells after combinatorial treatments was evaluated by resazurin assay. Briefly, resazurin solution (0.1 mg/ ml, Sigma) was added to cells at the end of each time point followed by incubation at 37 °C for 3 h. Eventually, the absorbance (A) of cells was measured at 600 nm by a microplate reader (Epoch), and the formula used for calculation of cell viability (%) was as $(100-(A_I-A_U/A_B-A_U)) \times 100$, in which A_I, A_U and A_B were A of treated cells, untreated cells and blank control, respectively.

The mode of interaction between urolithins and IR was assessed using the Chou-Talalay method. For this analysis, CompuSyn 1.0 software was employed to calculate the combination index (CI) and dose reduction index (DRI) parameters. The CI values obtained from the combinational treatments indicate the nature of the interactions, as $CI < 0.5$ reflects strong synergy, $0.5 \leq CI < 1$ signifies weak synergy, $CI = 1$ indicates additive effect, and $CI > 1$ reflects antagonism. The DRI parameter measures the extent of dose reduction in the combined therapy compared to single-agent treatment. A higher DRI value suggests a more significant reduction in treatment doses required to achieve cytotoxic effects, which is particularly advantageous in cancer therapy.

Interactome Mapping, Gene set Enrichment Analyses and Validating CHEK1 Expression

To investigate the importance of CHK1 and construct its protein-protein interaction network, related proteins in "response to DNA damage pathway from the Biocarta Pathways dataset" were retrieved from Harmonizome 3.0 (https://maayanlab.cloud/Harmonizome/gene_set). Subsequently, STRING database (https://string-db.org/) was utilized for interactome mapping of eight targets. Gene set enrichment analyses were performed in STRING in terms of Reactome pathways and WikiPathways and results yielded false discovery rate (FDR).

To validate the expression of CHEK1 in GA samples compared to normal specimens, GEPIA 2.0 (http://gepia2.cancer-pku.cn/) was utilized, which leverages data from the TCGA and GTEx databases. Additionally, to assess the expression of CHEK1 in MKN-45 cells, microarray data (GSE15460) were collected from GEO (http://www.ncbi.nlm.nih.gov/geo), which is a public repository containing high-throughput functional genomic data. Analysis was performed using R (version 4.4.0) with the "GEOquery" and "limma" packages. The p values were adjusted using the Benjamini & Hochberg method to control FDR. The volcano plot was generated using the "ggplot2" package in R, with a significance threshold of $p < .05$ and a $\log_2$ fold change ($\log_2$FC) > 0.5.

Molecular Docking

To predict the interactions between urolithins and CHK1, molecular docking was performed using AutoDock Vina program. The crystal structure of CHK1 (ID:3TKH) was retrieved from PDB Bank (http://www.rcsb.org/pdb), and the 3D structures of UroA (CID: 5488186) and UroB (CID: 5380406) were obtained from PubChem (https://pubchem.ncbi.nlm.nih.gov/). For mUroA, SMILE code was generated by Mathpix (https://snip.mathpix.com/home) and the SDF file was obtained from the National Cancer Institute's website (https://cactus.nci.nih.gov/translate/). AutoDockTools 1.5.7 was employed to assign polar hydrogens and atomic charges, and a grid box was specifically set to encompass the ATP binding pocket of CHK1. Finally, 2D and 3D diagrams were visualized using Discovery Studio.

Statistical Analysis

The results were statistically analyzed using GraphPad Prism 9.4.1, employing One-way ANOVA and Dunnet's multiple tests. All experiments were conducted in triplicate, and the results are presented as mean ± standard deviation (SD). *p*-values of less than .05, .01, .001, and .0001 were deemed statistically significant.

Results

The present study aimed to investigate whether pretreatment of GA cells with urolithins could enhance the efficacy of IR. Hence, MKN-45 cells were initially treated with increasing concentrations of urolithins alone, to determine the optimal concentration for combinatorial treatment. The calculated IC_{50} values for UroA, UroB and mUroA after 72 h were 92.7 μM, 110.5 μM and 155.5 μM, respectively. Therefore, 75 μM was selected as an optimal dose, since it was below the IC_{50} values of all three agents. To determine combined effects of urolithins and IR, cells were pretreated with 75 μM UroA, UroB and mUroA for 24, 48 and 72 h, then exposed to 400, 600 and 800 cGy IR and recovered for 48 and 24 h. As illustrated in Figure 1, pretreatment with UroA and mUroA for 24 h significantly ($p < .0001$ and $p < .001$) reduced viability after IR exposure. The most considerable decrease in the cell viability was observed upon exposure to 400 cGy IR. In comparison to the DMSO control treatment (96.7 ± 3.3%), 24 h pretreatment with UroA and mUroA reduced cell viability to 57.4 ± 7.1% and 62.8 ± 6.7%, respectively.

Figure 2 presents results of viability assay when cells were pretreated with urolithins for 48 h, irradiated at 400, 600 and 800 cGy and recovered for 48 h. As depicted, UroA and mUroA significantly ($p < .001$ and $p < .01$) reduced viability to 69.7 ± 1.2% and 72.7 ± 3.35% when exposed to 400 cGy IR, respectively. Furthermore, pretreatment of cells with UroA followed by 800 cGy IR induced significant ($p < .0001$) reduction in viability.

As presented in Figure 3, pretreatment with UroA, UroB and mUroA for 72 h significantly ($p < .01$) diminished viability upon IR exposure, and the most considerable reduction in cell viability was observed after 400 cGy radiotherapy. In comparison to the control treatments, 72 h pretreatment with UroA, UroB and mUroA reduced cell viability to 55.7 ± 11.2%, 56.3 ± 11.03% and 62.7 ± 0.04%, respectively.

The results of viability assay were corroborated by changes in cell morphology and density (Figure 4). Compared to control cells, which were 24 h pretreated with 0.4% DMSO followed by 400 cGy IR exposure, a reduced number of attached and viable cells were observed after 24 h pretreatment with UroA and mUroA followed by 400 cGy IR exposure and 48 h recovery.

To determine the interaction between urolithins and radiotherapy, CI and DRI values were calculated. As presented in Table 1, pretreatment with mUroA (24 h) followed by IR exposure (400, 600 and 800 cGy) demonstrated strong synergistic effects. Additionally, 24 h pretreatment with UroA induced weak synergistic effects with all IR doses. UroB, however, exhibited antagonistic effects in all combinatorial treatments. Regarding 48 h pretreatment with urolithins, only mUroA induced weak synergistic effects with 400 and 600 cGy IR. Similarly, upon 72 h pretreatment with urolithins, only mUroA induced weak synergistic

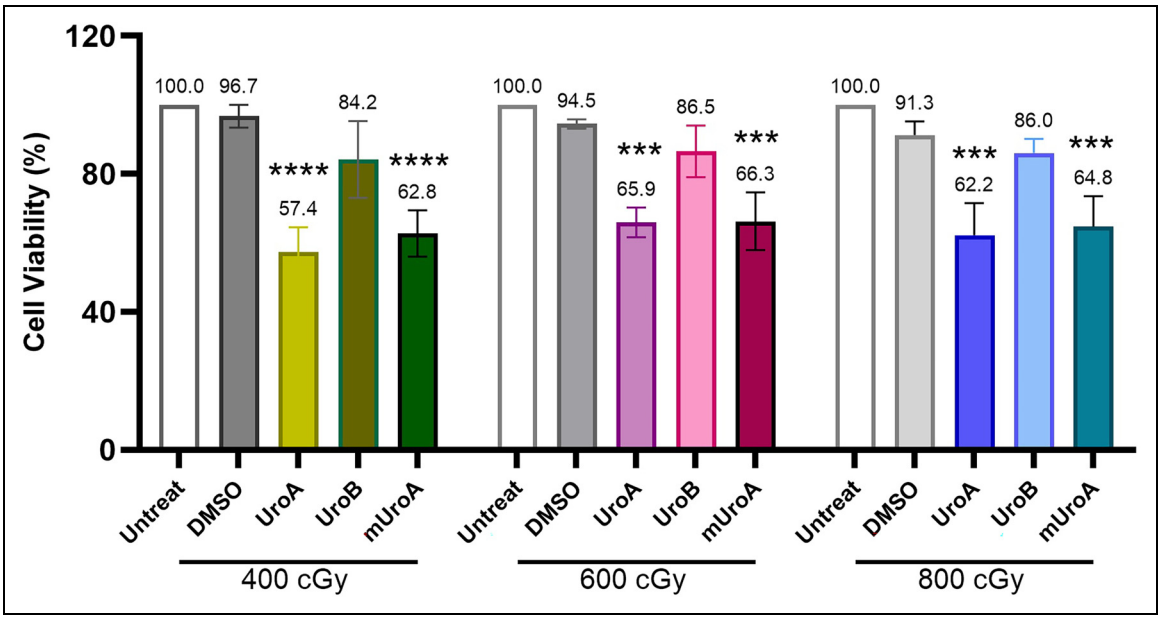

Figure 1. Viability of MKN-45 cells upon combinatorial treatment with urolithins and different doses of IR in comparison with relevant controls. Following 24 h pretreatment of cells with 75 μM UroA, UroB and mUroA, IR was applied at 400 cGy (A), 600 cGy (B) and 800 cGy (C), and then cells were recovered for 48 h. ***$p < .001$ and ****$p < .0001$ indicate significant difference with untreated and 0.4% DMSO controls. Results are presented as mean ± SD.

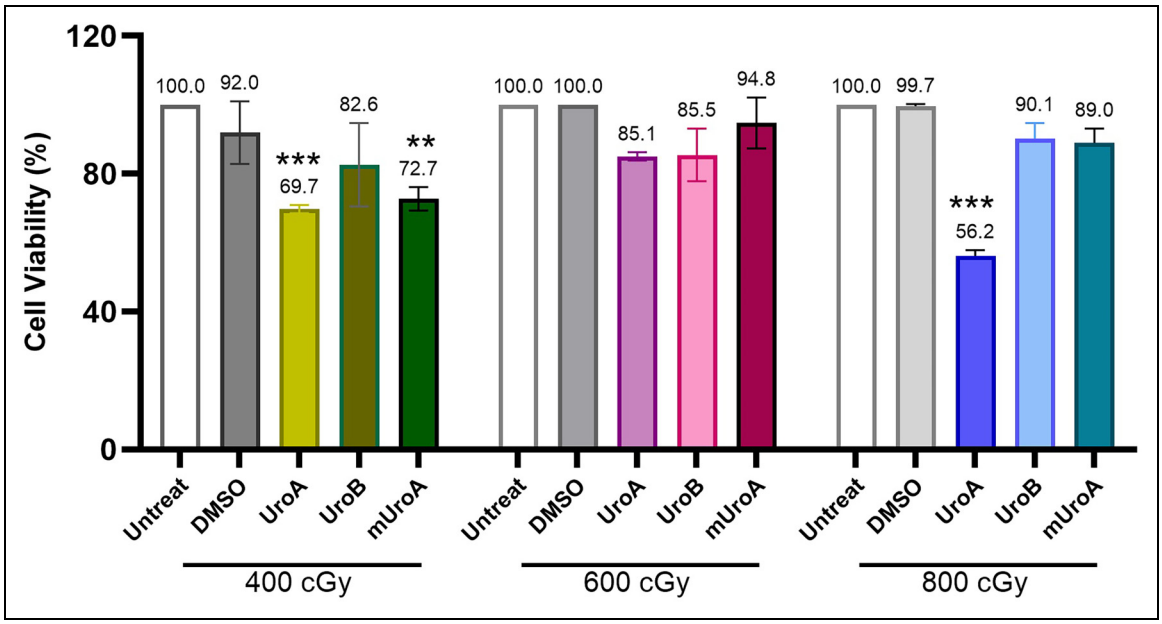

Figure 2. Viability of MKN-45 cells after combinatorial treatment with urolithins and IR in comparison with relevant controls. Upon 48 h pretreatment of cells with 75 μM UroA, UroB and mUroA, IR was applied at 400 cGy (A), 600 cGy (B) and 800 cGy (C), and then cells were recovered for 48 h. $^{**}p < .01$ and $^{***}p < .001$ indicate significant difference with untreated and 0.4% DMSO controls. Results are presented as mean ± SD.

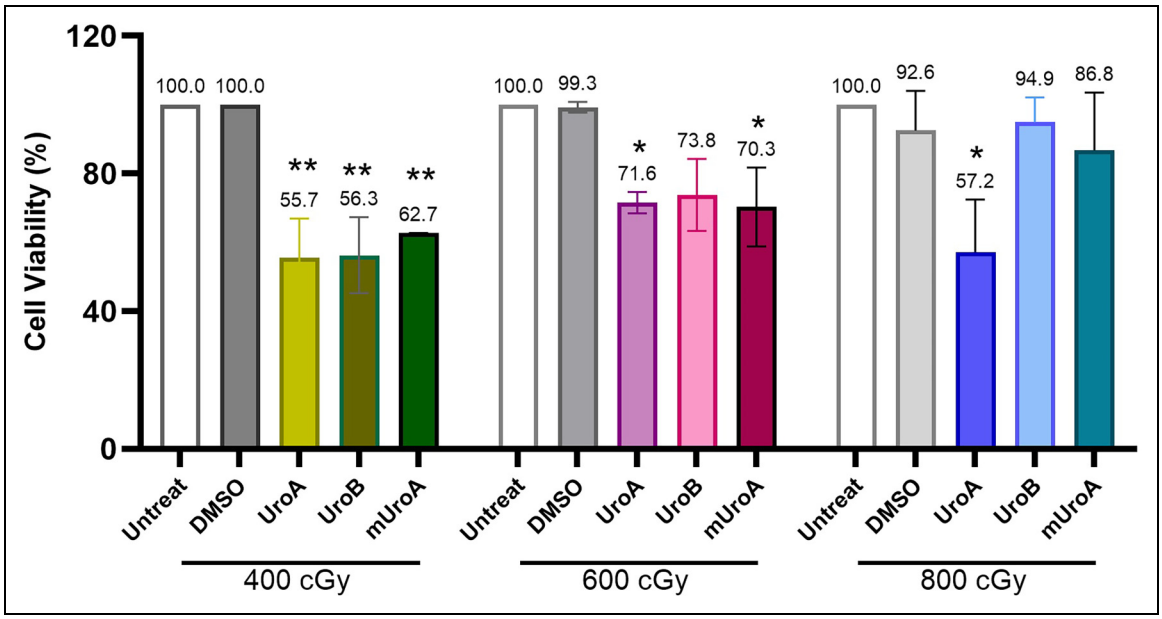

Figure 3. Viability of MKN-45 cells upon combinatorial treatment with urolithins and different doses of IR in comparison with relevant controls. Following 72 h pretreatment of cells with 75 μM UroA, UroB and mUroA, IR was applied at 400 cGy (A), 600 cGy (B) and 800 cGy (C), and then cells were recovered for 24 h. $^{*}p < .05$ and $^{**}p < .01$ indicate significant difference with untreated and 0.4% DMSO controls. Results are presented as mean ± SD.

effects with 400 cGy IR. The highest DRI values were calculated for UroA, as 24 h pretreatment with UroA followed by 400, 600 and 800 cGy radiotherapy resulted in 10.6-fold, 5.39-fold and 4.49-fold reduction in IR dose, respectively.

Web-based analysis revealed eight related targets for "cdc25 and chk1 regulatory pathway in response to DNA damage", including CHEK1, ATM, CDC25, CDK1, MYT1, WEE1, YWHAH and RASGRF1. As presented in Figure 5A, the

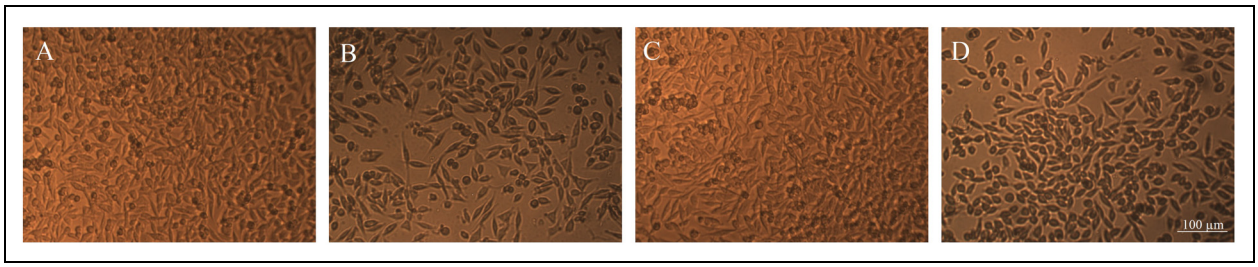

Figure 4. Morphological alteration of MKN-45 cells after pretreatment with urolithins and IR exposure. Phase contrast photomicrographs of cells pretreated with 0.4% DMSO (A) and 75 µM UroA (B), UroB (C) and mUroA (D) followed by exposure to 400 cGy IR and 48 h recovery.

Table 1. CI and DRI Values for Combinatorial Treatment of MKN-45 Cells upon 24, 48, and 72 h Pretreatment with Urolithins Followed by IR Exposure.

		400 cGy			600 cGy			800 cGy		
		Fa*	CI	DRI	Fa*	CI	DRI	Fa*	CI	DRI
UroA	24 h pretreatment, 48 h recovery	0.43	0.72	10.6	0.35	0.98	5.39	0.38	0.95	4.49
UroB		0.16	1.64	3.48	0.14	1.94	2.04	0.14	2.1	1.53
mUroA		0.38	0.31	8.98	034	0.53	5.2	0.36	0.5	4.19
UroA	48 h pretreatment, 48 h recovery	0.3	1.2	3.41	0.15	1.69	1.7	0.44	1.33	2.07
UroB		0.18	1.61	2.91	0.15	1.9	1.81	0.1	2.39	1.16
mUroA		0.26	0.8	3.2	0.06	0.88	1.22	0.11	1.02	1.14
UroA	72 h pretreatment, 24 h recovery	0.45	1.1	4.21	0.29	1.45	2.24	0.43	1.37	2.05
UroB		0.44	1.11	4.46	0.27	1.52	2.31	0.05	2.99	0.91
mUroA		0.38	0.76	3.83	0.3	1.09	2.27	0.14	2.09	1.24

*Fa: fraction of affected cells.

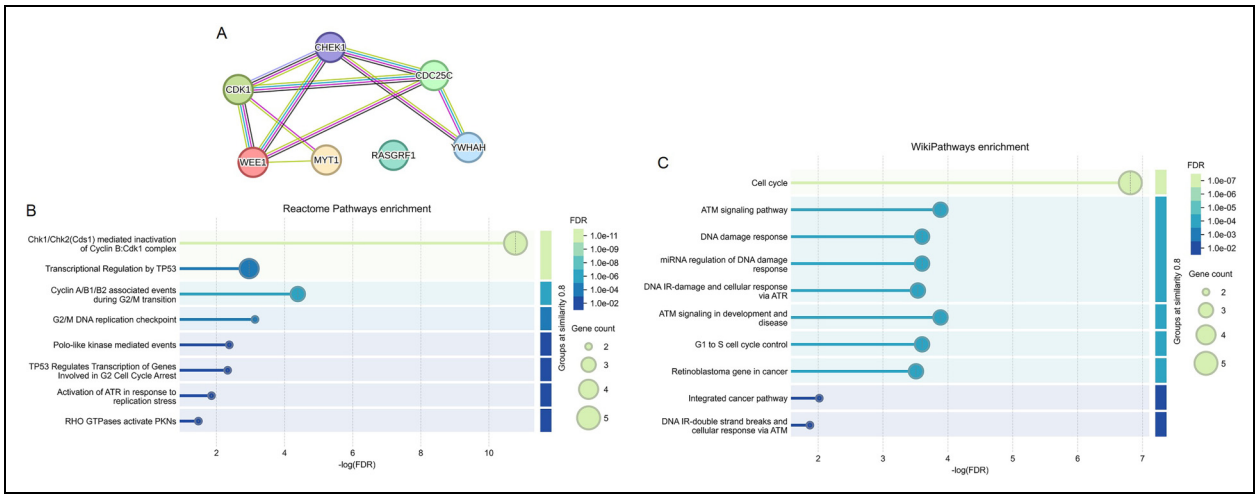

Figure 5. Interactome mapping and gene set enrichment analyses. STRING was used to map the inter-connectedness of related targets for "cdc25 and chk1 regulatory pathway in response to DNA damage (A). Gene ontology enrichment analyses identified significant terms in Reactome pathways (B) and WikiPathways (C).

protein-protein interaction network in STRING consisted of 7 nodes and 10 edges, with *p* value 2.01e-07. The enrichment analyses revealed significant terms in Reactome pathways and WikiPathways (Figure 5B and C). "Chk1/Chk2(Cds1) mediated inactivation of Cyclin B:Cdk1 complex" (FDR: 1.6e-11) and "G_2/M checkpoint " (FDR: 7.4e-4) were identified as significant terms in Reactome pathways. "DNA damage response" (FDR: 2.5e-4) and "DNA IR-damage and cellular response via ATR" (FDR: 2.9e-4) were among the most significant terms in WikiPathways.

As shown in Figure 6, validating the expression level of CHEK1 in GA patients via GEPIA2 revealed significant

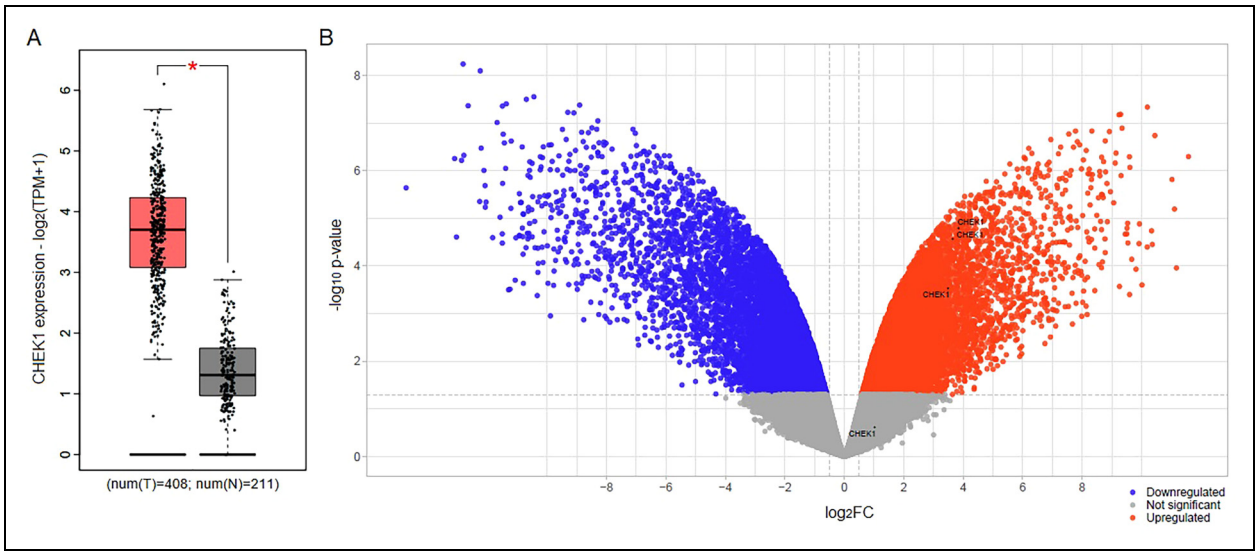

Figure 6. Validating the expression of CHEK1 in GA samples and cells. Box plot obtained from GEPIA2 (A) illustrates significant (*$p < .05$) overexpression of CHEK1 in GA tissue samples (N = 408) compared to normal specimens (N = 211). The volcano plot resulting from the differential expression analysis of GSE15460 (B) shows significant ($p < .05$ and $\log_2FC > 0.5$) upregulation of CHEK1 in MKN-45 cells compared to normal fibroblasts.

($p < .05$) overexpression in tumor tissues (n = 408) compared to normal samples (n = 211). Additionally, the expression of CHEK1 was investigated in MKN-45 cells compared to normal fibroblasts using GSE15460, and analysis revealed CHEK1 as an upregulated gene.

Since *in vitro* viability assay revealed synergistic effects of urolithins with IR, and computational analyses indicated elevated expression of CHEK1 in GA samples and MKN-45 cells, we investigated whether combinatorial effects of urolithins and IR were due to their interaction with CHK1. Results of molecular docking indicated bindings of urolithins within the ATP binding pocket of CHK1. The interaction between UroA and CHK1 was stable and involved three hydrogen bonds with LYS38, GLU85, and ASP148 with a binding energy of −7.8 kcal/mol (Figure 7A). The interaction between UroB and CHK1 involved two hydrogen bonds with residues LYS38 and GLU85 and exhibited a binding energy of −6.3 kcal/mol (Figure 7B). Interestingly, the interaction between mUroA and CHK1 involved three covalent (C-H) bonds with GLU85 and SER147 and one hydrogen bond with ASP148 with a binding energy of −6.6 kcal/mol (Figure 7C).

Discussion and Conclusion

GA is the fourth leading cause of cancer-related mortality worldwide.[1] The early diagnosis of this neoplasm is often hindered by the absence of clear clinical symptoms, resulting in most patients being diagnosed at advanced stages, which correlates with a poor prognosis of less than one year.[6] While various treatment approaches have shown potential benefits for GA, challenges such as acquired resistance and off-target toxicity continue to pose significant hurdles.[13] In light of the inadequate clinical responses to radiotherapy, there is a growing emphasis on utilizing natural agents with radiosensitizing effects. Our previous studies demonstrated that natural coumarins, including auraptene, umbelliprenin and galbanic acid, enhanced the efficacy of radiotherapy in leukemia/lymphoma as well as gastric and colon carcinoma cells.[45-50]

Gut microbiota plays a crucial role in maintaining homeostasis by regulating digestion, metabolism, and immune function, thereby preventing dysbiosis and reducing the risk of chronic diseases while supporting overall physiological stability and health.[51-55] As gut microbiota metabolites, urolithins are associated with various health benefits, and interestingly, research has shown that direct supplementation can significantly increase plasma levels of urolithins, effectively overcoming the challenges posed by dietary variability. Urolithins, primarily found in plasma as glucuronide and sulfate conjugates, typically exhibit concentrations ranging around 20 μM following dietary intake.[19,56,57] However, when considering the potential use of urolithins as radiosensitizers, local injection may offer advantages over systemic administration. By delivering urolithins directly to the tumor site, higher concentrations can be achieved, potentially enhancing their therapeutic effects in combination with IR. This localized approach could maximize the synergistic effects of urolithins while minimizing systemic exposure and associated side effects.

In addition to their potential protective roles against chronic diseases, urolithins also demonstrate significant anticancer activity. Examining the effects of urolithins on breast, colon, pancreatic, liver, prostate and bladder carcinoma cells revealed that they exert anticancer activity through multiple mechanisms, including the induction of cell cycle arrest and apoptosis, activation of P38-MAPK and caspase-3, reduction of oxidative stress, and

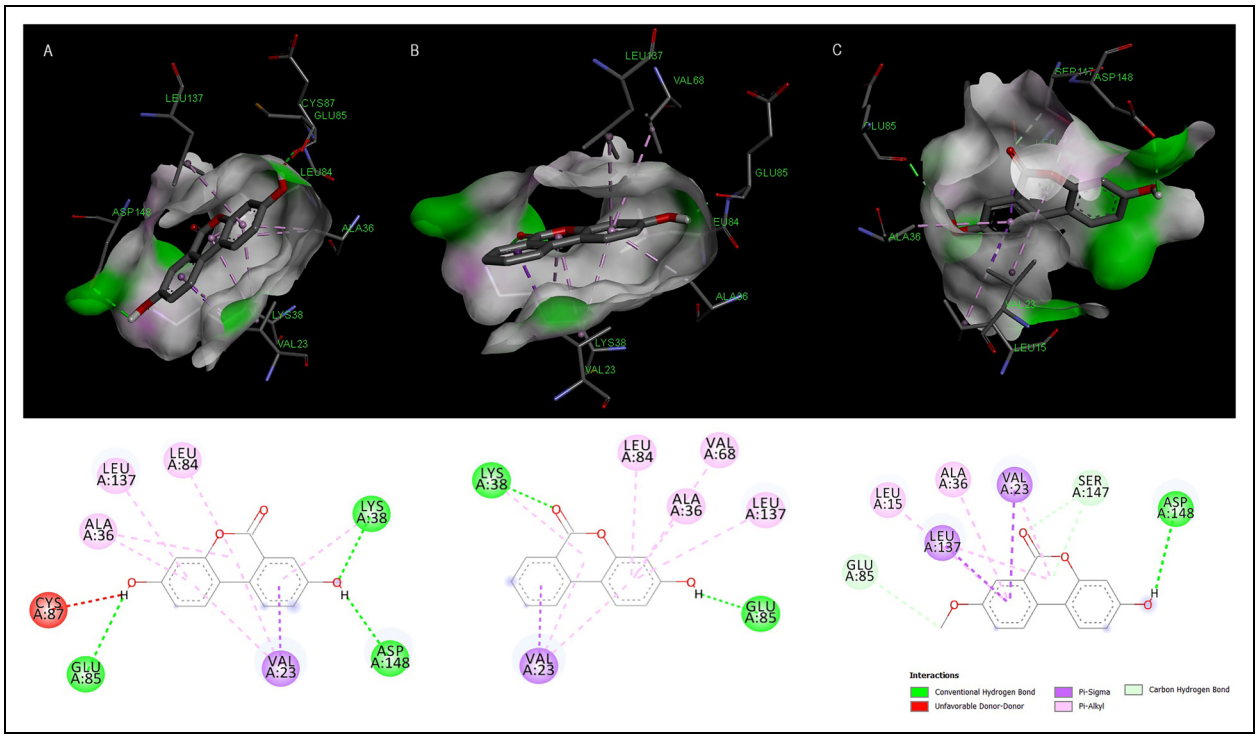

Figure 7. Molecular docking diagrams of urolithins interacting with CHK1. The interactions are presented for UroA (A), UroB (B) and mUroA (C) in the ATP binding pocket of CHK1. Both 2D and 3D images were generated by Discovery Studio.

regulation of P21, P53, c-MYC, CDKN1A, RB1, AKT, and β-catenin.[24,30,58-61] A recent study has demonstrated that UroA inhibited the proliferation, migration, and invasion of GA cells while promoting apoptosis and autophagy.[62] Limited research has been conducted on the synergistic and combinatorial effects of urolithins with anticancer modalities. One study reported that combination of UroA and 5-(3′,4′,5′-trihydroxyphenyl)-γ-valerolactone induced synergistic anti-proliferative effects on prostate carcinoma cells.[25] Additionally, combination of UroA with 5-fluorouracil reduced the viability and invasion of colon adenocarcinoma cells.[41] Furthermore, our previous research has reported enhanced efficacy of chemotherapy with paclitaxel and cisplatin, radiotherapy, and thermal therapy, when combined with urolithins in esophageal carcinoma cells.[42] Findings of the present study provided the first evidence that pretreatment of GA cells with urolithins enhanced efficacy of radiotherapy. Investigating the interaction between urolithins and IR revealed that UroA and, notably, mUroA induced synergistic effects with 400 and 600 cGy radiation, unlike UroB, which did not exhibit this enhancement. Notably, the administration of 400–800 cGy IR is consistent with clinical applications, as trials have demonstrated that this range of radiation can be effective in achieving tumor control and enhancing the efficacy of concurrent therapies in various cancers.[63-65] The increased efficacy of mUroA compared to other urolithins is primarily due to its chemical structure, featuring an additional methyl group that enhances lipophilicity. This property improves its ability to penetrate cell membranes, resulting in higher intracellular concentrations and stronger biological effects. Additionally, methylation enhances stability and bioavailability, allowing mUroA to persist longer in biological systems. Furthermore, methylated form of urolithin may exhibit altered interactions with cellular targets, potentially increasing its affinity for molecules involved in DDR, and this hypothesis is supported by the results of our molecular docking analysis.

CHK1 is a pivotal regulator of the DDR that, upon DNA damage, undergoes phosphorylation and activation, leading to cell cycle arrest. This mechanism provides cells with the necessary time to repair DNA before proceeding with mitosis, thereby preserving genomic integrity, especially under stress conditions such as those induced by IR. Given its critical role in promoting cell survival following DNA damage, CHK1 has emerged as a promising therapeutic target in cancer treatment. Inhibiting CHK1 can sensitize cancer cells to DNA-damaging agents, including chemotherapy and radiotherapy, by impairing their capacity to effectively repair DNA damage.[15,17,18] Computational analyses in the current study provided a deeper understanding of combinatorial effects of urolithins and radiotherapy. The protein-protein interaction network consisted main proteins in the regulatory pathway in response to DNA damage, including CHK1. The low FDR value of "DNA IR-damage and cellular response via ATR" in WikiPathways underscores the importance of CHK1 as a potential therapeutic target to improve DNA damaging effects of IR. In consistence with our findings, research has

demonstrated that the cytotoxicity of CHK1 inhibitors is linked to the induction of DNA damage, which ultimately results in apoptosis, mitotic slippage, and permanent cell cycle arrest.[66]

Upregulated expression of CHEK1 in GA tissue samples underscores the importance of developing novel agents that can interact with CHK1 activity. Moreover, elevated expression of CHEK1 in MKN-45 cells indicated that this cell line could be considered as a suitable model to study CHK1 expression and activity. The ATP binding pocket of CHK1 features several key amino acids, including LEU84, GLU85, and ASP148.[67,68] Molecular docking analysis revealed that urolithins favorably interacted with these residues with strong binding affinities. Notably, the interaction between mUroA and the ATP binding pocket of CHK1 was particularly intriguing, involving the formation of three covalent bonds and one hydrogen bond, which was greater than that observed with UroA and UroB. This finding correlates with the enhanced combinatorial effects noted in our combinatorial treatments *in vitro*. To date, only a few small molecules like UCN-01 have been identified as CHK1 inhibitors that interact with the ATP binding site of CHK1.[69] In light of this, our findings suggest for the first time that urolithins—metabolites produced by gut microbiota—have significant potential to enhance the efficacy of radiotherapy by inhibiting CHK1 activity. This discovery holds exciting promise for the development of new natural radiosensitizers.

The present study has certain limitations that warrant further investigation. To fully validate the findings from our *in vitro* and *in silico* analyses and to better elucidate the precise molecular mechanisms underlying the synergistic action of urolithins and radiotherapy, experiments on other GA cell lines and animal models is recommended. Furthermore, exploring urolithin metabolites and evaluating the effects of urolithins in combination with other therapeutic modalities will provide a more comprehensive perspective on their potential benefits. Additionally, utilizing *ex vivo* methods to get the metabolite of the natural products could provide deeper insights into their biological effects as they occur in a natural context.

Authors' Contribution

AR. Ahmadi F. Hosseini and H. Ostadi carried out the experiments and analyses of the results, H. Gholamhosseinian performed radiotherapy, M. Iranshahy synthesized urolithins and F.B. Rassouli contributed to the design and supervision of the project and revision of the manuscript.

Data Availability

The data that support the findings of this study are available on request from the corresponding authors.

Declaration of Conflicting Interests

The authors declared no potential conflicts of interest with respect to the research, authorship, and/or publication of this article.

Ethical Approval

Ethical Approval is not applicable for this article.

Funding

The author(s) disclosed receipt of the following financial support for the research, authorship, and/or publication of this article: This study was supported by Ferdowsi University of Mashhad, Mashhad, Iran.

Statement of Human and Animal Rights

Ethical Approval is not applicable for this article.

Statement of Informed Consent

Ethical Approval is not applicable for this article.

ORCID iD

Fatemeh B. Rassouli https://orcid.org/0000-0003-1889-0964

References

1. Sung H, Ferlay J, Siegel RL, et al. Global cancer statistics 2020: GLOBOCAN estimates of incidence and mortality worldwide for 36 cancers in 185 countries. *CA Cancer J Clin*. 2021;71(3):209-249. doi: 10.3322/caac.21660
2. Bray F, Ferlay J, Soerjomataram I, Siegel RL, Torre LA, Jemal A. Global cancer statistics 2018: GLOBOCAN estimates of incidence and mortality worldwide for 36 cancers in 185 countries. *CA Cancer J Clin*. 2018;68(6):394-424. doi: 10.3322/caac.21492
3. Hess T, Maj C, Gehlen J, et al. Dissecting the genetic heterogeneity of gastric cancer. *EBioMedicine*. 2023;92(18):104616. doi: 10.1016/j.ebiom.2023.104616
4. Zhou Z, Jiang Y, Sun Z, et al. Virtual multiplexed immunofluorescence staining from non-antibody-stained fluorescence imaging for gastric cancer prognosis. *EBioMedicine*. 2024;107:105287. doi: 10.1016/j.ebiom.2024.105287
5. Zhao J, Han Z, Xu C, et al. Separation and single-cell analysis for free gastric cancer cells in ascites and peritoneal lavages based on microfluidic chips. *EBioMedicine*. 2023;90:104522. doi: 10.1016/j.ebiom.2023.104522
6. Hu HM, Tsai HJ, Ku HY, et al. Survival outcomes of management in metastatic gastric adenocarcinoma patients. *Sci Rep*. 2021;11(1):23142. doi: 10.1038/s41598-021-02391-z
7. Li Z, Wang J, Wang Z, Xu Y. Towards an optimal model for gastric cancer peritoneal metastasis: current challenges and future directions. *EBioMedicine*. 2023;92:104601. doi: 10.1016/j.ebiom.2023.104601
8. Guan WL, He Y, Xu RH. Gastric cancer treatment: recent progress and future perspectives. *J Hematol Oncol*. 2023;16(1):57. doi: 10.1186/s13045-023-01451-3
9. Yu J, Feng H, Sang Q, et al. VPS35 Promotes cell proliferation via EGFR recycling and enhances EGFR inhibitors response in gastric cancer. *EBioMedicine*. 2023;89:104451. doi: 10.1016/j.ebiom.2023.104451

10. Takeda K, Sakayauchi T, Kubozono M, et al. Palliative radiotherapy for gastric cancer bleeding: a multi-institutional retrospective study. *BMC Palliat Care*. 2022;21(1):52. doi: 10.1186/s12904-022-00943-2
11. Shinde A, Novak J, Amini A, Chen YJ. The evolving role of radiation therapy for resectable and unresectable gastric cancer. *Transl Gastroenterol Hepatol*. 2019;4:64. doi: 0.21037/tgh.2019.08.06
12. Smalley SR, Benedetti JK, Haller DG, et al. Updated analysis of SWOG-directed intergroup study 0116: a phase III trial of adjuvant radiochemotherapy versus observation after curative gastric cancer resection. *J Clin Oncol*. 2012;30(19):2327-2333. doi: 10.1200/JCO.2011.36.7136
13. Sitarz R, Skierucha M, Mielko J, Offerhaus GJA, Maciejewski R, Polkowski WP. Gastric cancer: epidemiology, prevention, classification, and treatment. *Cancer Manag Res*. 2018;10:239-248. doi: 10.2147/CMAR.S149619
14. Wang FZ, Fei HR, Cui YJ, et al. The checkpoint 1 kinase inhibitor LY2603618 induces cell cycle arrest, DNA damage response and autophagy in cancer cells. *Apoptosis*. 2014;19(9):1389-1398. doi: 10.1007/s10495-014-1010-3
15. Zhang Y, Hunter T. Roles of chk1 in cell biology and cancer therapy. *Int J Cancer*. 2014;134(5):1013-1023. doi: 10.1002/ijc.28226
16. Smith J, Tho LM, Xu N, Gillespie DA. The ATM-Chk2 and ATR-Chk1 pathways in DNA damage signaling and cancer. *Adv Cancer Res*. 2010;108:73-112. doi: 10.1016/B978-0-12-380888-2.00003-0
17. Höglund A, Nilsson LM, Muralidharan SV, et al. Therapeutic implications for the induced levels of Chk1 in myc-expressing cancer cells. *Clin Cancer Res*. 2011;17(22):7067-7079. doi: 10.1158/1078-0432.CCR-11-1198
18. Qiu Z, Oleinick NL, Zhang J. ATR/CHK1 inhibitors and cancer therapy. *Radiother Oncol*. 2018;126(3):450-464. doi: 10.1016/j.radonc.2017.09.043
19. García-Villalba R, Giménez-Bastida JA, Cortés-Martín A, et al. Urolithins: a comprehensive update on their metabolism, bioactivity, and associated gut microbiota. *Mol Nutr Food Res*. 2022;66(21):e2101019. doi: 10.1002/mnfr.202101019
20. Cortés-Martín A, Selma MV, Tomás-Barberán FA, González-Sarrías A, Espín JC. Where to look into the puzzle of polyphenols and health? The postbiotics and gut microbiota associated with human metabotypes. *Mol Nutr Food Res*. 2020;64(9):e1900952. doi: 10.1002/mnfr.201900952
21. Al-Harbi SA, Abdulrahman AO, Zamzami MA, Khan MI. Urolithins: the gut based polyphenol metabolites of ellagitannins in cancer prevention, a review. *Front Nutr*. 2021;8:647582. doi: 10.3389/fnut.2021.647582
22. Stolarczyk M, Piwowarski JP, Granica S, Stefańska J, Naruszewicz M, Kiss AK. Extracts from epilobium sp. Herbs, their components and gut microbiota metabolites of epilobium ellagitannins, urolithins, inhibit hormone-dependent prostate cancer cells-(LNCaP) proliferation and PSA secretion. *Phytother. Res*. 2013;27:1842-1848. doi: 10.1002/ptr.4941
23. Zhang W, Chen JH, Aguilera-Barrantes I, et al. Urolithin A suppresses the proliferation of endometrial cancer cells by mediating estrogen receptor-α-dependent gene expression. *Mol Nutr Food Res*. 2016;60:2387-2395. doi: 10.1002/mnfr.201600048
24. Dahiya NR, Chandrasekaran B, Kolluru V, Ankem M, Damodaran C, Vadhanam MV. A natural molecule, urolithin A, downregulates androgen receptor activation and suppresses growth of prostate cancer. *Mol Carcinog*. 2018;57(10):1332-1341. doi: 10.1002/mc.22848
25. Stanisławska IJ, Granica S, Piwowarski JP, et al. The activity of urolithin A and M4 valerolactone, colonic microbiota metabolites of polyphenols, in a prostate cancer in vitro model. *Planta Med*. 2019;85(2):118-125. doi: 10.1055/a-0755-7715
26. Totiger TM, Srinivasan S, Jala VR, et al. Urolithin A, a novel natural compound to target PI3K/AKT/mTOR pathway in pancreatic cancer. *Mol Cancer Ther*. 2019;18:301-311. doi: 10.1158/1535-7163.MCT-18-0464
27. Wang Y, Qiu Z, Zhou B, et al. In vitro antiproliferative and antioxidant effects of urolithin A, the colonic metabolite of ellagic acid, on hepatocellular carcinomas HepG2 cells. *Toxicol In Vitro*. 2015;29:1107-1115. doi: 10.1016/j.tiv.2015.04.008
28. Qiu Z, Zhou J, Zhang C, Cheng Y, Hu J, Zheng G. Antiproliferative effect of urolithin A, the ellagic acid-derived colonic metabolite, on hepatocellular carcinoma HepG2.2.15 cells by targeting Lin28a/let-7a axis. *Braz J Med Biol Res*. 2018;51:e7220. doi: 10.1590/1414-431x20187220
29. Sahashi H, Kato A, Yoshida M, et al. Urolithin A targets the AKT/WNK1 axis to induce autophagy and exert anti-tumor effects in cholangiocarcinoma. *Front Oncol*. 2022;12:963314. doi: 10.3389/fonc.2022.963314
30. Liberal J, Carmo A, Gomes C, Cruz MT, Batista MT. Urolithins impair cell proliferation, arrest the cell cycle and induce apoptosis in UMUC3 bladder cancer cells. *Invest New Drugs*. 2017;35(6):671-681. doi: 10.1007/s10637-017-0483-7
31. Qiu Z, Zhou B, Jin L, et al. In vitro antioxidant and antiproliferative effects of ellagic acid and its colonic metabolite, urolithins, on human bladder cancer T24 cells. *Food Chem Toxicol*. 2013;59:428-437. doi: 10.1016/j.fct.2013.06.025
32. Giménez-Bastida JA, Ávila-Gálvez MÁ, Espín JC, González-Sarrías A. The gut microbiota metabolite urolithin A, but not other relevant urolithins, induces p53-dependent cellular senescence in human colon cancer cells. *Food Chem Toxicol*. 2020;139:111260. doi: 10.1016/j.fct.2020.111260
33. González-Sarrías A, Espín JC, Tomás-Barberán FA, García-Conesa MT. Gene expression, cell cycle arrest and MAPK signalling regulation in caco-2 cells exposed to ellagic acid and its metabolites, urolithins. *Mol Nutr Food Res*. 2009;53:686-698. doi: 10.1002/mnfr.200800150
34. Kasimsetty SG, Bialonska D, Reddy MK, Ma G, Khan SI, Ferreira D. Colon cancer chemopreventive activities of pomegranate ellagitannins and urolithins. *J Agric Food Chem*. 2010;58:2180-2187. doi: 10.1021/jf903762h
35. Zhao W, Shi F, Guo Z, Zhao J, Song X, Yang H. Metabolite of ellagitannins, urolithin A induces autophagy and inhibits metastasis in human sw620 colorectal cancer cells. *Mol Carcinog*. 2018;57:193-200. doi: 10.1002/mc.22746
36. Shen CK, Huang BR, Charoensaensuk V, et al. Inhibitory effects of urolithins, bioactive gut metabolites from natural polyphenols,

against glioblastoma progression. *Nutrients*. 2023;15(23):4854. doi: 10.3390/nu15234854

37. Eidizade F, Soukhtanloo M, Zhiani R, Mehrzad J, Mirzavi F. Inhibition of glioblastoma proliferation, invasion, and migration by urolithin B through inducing G0/G1 arrest and targeting MMP-2/-9 expression and activity. *Biofactors*. 2023;49:379-389. doi: 10.1002/biof.1915
38. Cheng F, Dou J, Zhang Y, et al. Urolithin A inhibits epithelial-mesenchymal transition in lung cancer cells via P53-Mdm2-snail pathway. *Onco Targets Ther*. 2021;14:3199-3208. doi: 10.2147/OTT.S305595
39. Yang Y, Ren ZZ, Wei WJ, et al. Study on the biological mechanism of urolithin a on nasopharyngeal carcinoma in vitro. *Pharm Biol*. 2022;60(1):1566-1577. doi: 10.1080/13880209.2022.2106251
40. Alauddin M, Okumura T, Rajaxavier J, et al. Gut bacterial metabolite urolithin A decreases actin polymerization and migration in cancer cells. *Mol Nutr Food Res*. 2020;64(7):e1900390. doi: 10.1002/mnfr.201900390
41. Ghosh S, Singh R, Vanwinkle ZM, et al. Microbial metabolite restricts 5-fluorouracil-resistant colonic tumor progression by sensitizing drug transporters via regulation of FOXO3-FOXM1 axis. *Theranostics*. 2022;12(12):5574-5595. doi: 10.7150/thno.70754
42. Mirzaei S, Iranshahy M, Gholamhosseinian H, Matin MM, Rassouli FB. Urolithins increased anticancer effects of chemical drugs, ionizing radiation and hyperthermia on human esophageal carcinoma cells in vitro. *Tissue Cell*. 2022;77:101846. doi: 10.1016/j.tice.2022.101846
43. Bialonska D, Kasimsetty SG, Khan SI, Ferreira D. Urolithins, intestinal microbial metabolites of pomegranate ellagitannins, exhibit potent antioxidant activity in a cell-based assay. *J Agric Food Chem*. 2009;57(21):10181-10186. doi:10.1021/jf9025794
44. Hristov B, Lin SH, Christodouleas JP. *Radiation Oncology: A Question-Based Review*. 3rd ed. Lippincott Williams & Wilkins; 2018, ISBN: 978-1-49-636036-6.
45. Bagheri R, Rassouli FB, Gholamhosseinian H, et al. Radiation response of human leukemia/lymphoma cells was improved by 7-geranyloxycoumarin. *Dose Response*. 2022;20(3):15593258221124479. doi: 10.1177/15593258221124479
46. Salari H, Afkhami-Poostchi A, Soleymanifard S, et al. Coadministration of auraptene and radiotherapy; a novel modality against colon carcinoma cells in vitro and in vivo. *Int J Radiat Biol*. 2020;96(8):1051-1059. doi: 10.1080/09553002.2020.1770359
47. Movaffagh J, Salari H, Merajifar E, et al. 7-geranyloxycoumarin Enhanced radiotherapy effects on human gastric adenocarcinoma cells. *J Cancer Res Ther*. 2023;19(3):590-594. doi: 10.4103/jcrt.jcrt_701_21
48. Moussavi M, Haddad F, Rassouli FB, Iranshahi M, Soleymanifard S. Synergy between auraptene, ionizing radiation, and anticancer drugs in colon adenocarcinoma cells. *Phytother Res*. 2017;31(9):1369-1375. doi: 10.1002/ptr.5863
49. Ebrahimi K, Bagheri R, Gholamhosseinian H, et al. Umbelliprenin improved anti-proliferative effects of ionizing radiation on adult T-cell leukemia/lymphoma cells via interaction with CDK6; an in vitro and in silico study. *Int J Immunopathol Pharmacol*. 2024;38:3946320241287873. doi: 10.1177/03946320241287873
50. Farahi M, Hashemi R, Rassouli FB, Iranshahi M, Soleymanifard S. Investigation of the toxic effects of galbanic acid with ionizing radiation on human colon cancer HT-29 cells. *Pharm Chem J*. 2023;57:408-413. doi.org/10.1007/s11094-023-02898-x
51. Singh R, Chandrashekharappa S, Bodduluri SR, et al. Enhancement of the gut barrier integrity by a microbial metabolite through the Nrf2 pathway. *Nat Commun*. 2019;10(1):89. doi: 10.1038/s41467-018-07859-7
52. Zhang Y, Chen R, Zhang D, Qi S, Liu Y. Metabolite interactions between host and microbiota during health and disease: which feeds the other? *Biomed Pharmacother*. 2023;160:114295. doi: 10.1016/j.biopha.2023.114295
53. Kim S, Seo SU, Kweon MN. Gut microbiota-derived metabolites tune host homeostasis fate. *Semin Immunopathol*. 2024;46:2. doi.org/10.1007/s00281-024-01012-x
54. Wu Y, Feng X, Li M, et al. Gut microbiota associated with appetite suppression in high-temperature and high-humidity environments. *EBioMedicine*. 2024;99:104918. doi: 10.1016/j.ebiom.2023.104918
55. Zeng W, Wu J, Xie H, et al. Enteral nutrition promotes the remission of colitis by gut bacteria-mediated histidine biosynthesis. *EBioMedicine*. 2024;100:104959. doi: 10.1016/j.ebiom.2023.104959
56. Singh A, D'Amico D, Andreux PA, et al. Direct supplementation with urolithin A overcomes limitations of dietary exposure and gut microbiome variability in healthy adults to achieve consistent levels across the population. *Eur J Clin Nutr*. 2022;76(2):297-308. doi: 10.1038/s41430-021-00950-1
57. Espín JC, Larrosa M, García-Conesa MT, Tomás-Barberán F. Biological significance of urolithins, the gut microbial ellagic acid-derived metabolites: the evidence so far. *Evid Based Complement Alternat Med*. 2013;2013:270418. doi: 10.1155/2013/270418
58. Avila-Gálvez MÁ, Espín JC, González-Sarrías A. Physiological relevance of the antiproliferative and estrogenic effects of dietary polyphenol aglycones versus their phase-II metabolites on breast cancer cells: a call of caution. *J Agric Food Chem*. 2018;66(32):8547-8555. doi: 10.1021/acs.jafc.8b03100
59. Norden E, Heiss EH. Urolithin A gains in antiproliferative capacity by reducing the glycolytic potential via the p53/TIGAR axis in colon cancer cells. *Carcinogenesis*. 2019;40(1):93-101. doi: 10.1093/carcin/bgy158
60. Mehra S, Garrido VT, Dosch AR, et al. Remodeling of stromal immune microenvironment by urolithin A improves survival with immune checkpoint blockade in pancreatic cancer. *Cancer Res Commun*. 2023;3(7):1224-1236. doi.org/10.1158/2767-9764.CRC-22-0329
61. Lv MY, Shi CJ, Pan FF, et al. Urolithin B suppresses tumor growth in hepatocellular carcinoma through inducing the inactivation of Wnt/β-catenin signaling. *J Cell Biochem*. 2019;120(10):17273-17282. doi: 10.1002/jcb.28989
62. Zhang Y, Jiang L, Su P, et al. Urolithin A suppresses tumor progression and induces autophagy in gastric cancer via the PI3K/Akt/mTOR pathway. *Drug Dev Res*. 2023;84(2):172-184. doi: 10.1002/ddr.22021
63. Yang Y, Xu X, Zhou X, et al. Impact of radiation dose on survival for esophageal squamous cell carcinoma treated with neoadjuvant

chemoradiotherapy. *Front Oncol*. 2020;10:1431. doi: 10.3389/fonc.2020.01431

64. Venkatesulu BP, Sharma A, Pollard-Larkin JM, et al. Ultra high dose rate (35 Gy/sec) radiation does not spare the normal tissue in cardiac and splenic models of lymphopenia and gastrointestinal syndrome. *Sci Rep*. 2019;9(1):17180. doi: 10.1038/s41598-019-53562-y
65. Kong FM, Zhao J, Wang J, Faivre-Finn C. Radiation dose effect in locally advanced non-small cell lung cancer. *J Thorac Dis*. 2014;6(4):336-347. doi: 10.3978/j.issn.2072-1439.2014.01.23
66. Wayne J, Brooks T, Massey AJ. Inhibition of Chk1 with the small molecule inhibitor V158411 induces DNA damage and cell death in an unperturbed S-phase. *Oncotarget*. 2016;7(51):85033-85048. doi: 10.18632/oncotarget.13119
67. Caparelli ML, O'Connell MJ. Regulatory motifs in Chk1. *Cell Cycle*. 2013;12(6):916-922. doi: 10.4161/cc.23881
68. Kornelia C, Jacek K, Karol K, Marek K. Bernard selected arylsulphonyl pyrazole derivatives as potential Chk1 kinase ligands—computational investigations. *J Mol Model*. 2020;26(6):144. doi: 10.1007/s00894-020-04407-3
69. Zhao B, Bower MJ, McDevitt PJ, et al. Structural basis for Chk1 inhibition by UCN-01. *J Biol Chem*. 2002;277(48):46609-46615. doi: 10.1074/jbc.M201233200